Seismic and geodetic constraints on Cascadia slow slip

Aaron G. Wech[1], Kenneth C. Creager[1], & Timothy I. Melbourne[2]

[1]*University of Washington, Department of Earth and Space Science, Box 351310, Seattle, WA, 98195, USA.*

[2]*Central Washington University, Department of Geological Sciences, Ellensburg, WA, 98926, USA.*

Abstract: Automatically detected and located tremor epicenters from episodic tremor and slip (ETS) episodes in northern Cascadia provide a high-resolution map of Washington's slow slip region. Thousands of epicenters from each of the past four ETS events from 2004—2008 provide detailed map-view constraints that correlate with geodetic estimates of the simultaneous slow slip activity. Analysis of the latest 15-month inter-ETS period also reveals ageodetic tremor activity similar both in duration and extent to ETS tremor. Epicenters from both ETS and inter-ETS tremor are bounded between the 30—45 km plate interface depth contours and locate approximately 75 km east of previous estimates of the locked portion of the subducting Juan de Fuca plate. Based on the high spatio-temporal correlation between tremor and slip, the tremor duration and slip magnitude relationship and the similarity in map view and duration of ETS and inter-ETS tremor, we suggest that the well-resolved, sharp updip edge of tremor epicenters reflects a change in plate interface coupling properties. This region updip of the tremor epicenter boundary likely accumulates stress with the potential for coseismic shear failure during a megathrust earthquake. Alternatively, slip in this region could be accommodated by slow slip events with sufficiently long recurrence intervals that none have been detected during the past 10 years of GPS observations.

1. Introduction

The region of Cascadia extending from northern California to northern Vancouver Island is tectonically characterized by the subduction of the oceanic Juan de Fuca plate beneath the continental North American plate. Geodetically inferred long-term deformation suggests strain accumulation in the overriding crust in response to the steady convergence of the subducting slab [*McCaffrey et al.*, 2008]. This deformation results from interseismic coupling along an offshore portion of the subducting plate interface, which is known to have exhibited multiple incidents of shear failure in the form of megathrust earthquakes up to magnitude 9 [*Satake et al.*, 2003; *Goldfinger et al.*, 2003]. Somewhere downdip of this seismogenic coupling and some zone of transition, however, the pressure, temperature, composition, and/or fluid environment at the plate interface enables the oceanic plate to freely subduct without any seismogenic coupling to the overriding continent. It is poorly understood, though, how and where this transition is realized. As a spatially constrainable mechanism for stable strain release, episodic tremor and slip (ETS) provides information about this transition region.

ETS in northern Cascadia is characterized by the repeated coincidence of seismically observed non-volcanic tremor activity [*Obara*, 2002] and geodetically observed slow slip [*Dragert et al*., 2001] every 14 ± 2 months [*Miller et al*., 2002; *Rogers and Dragert*, 2003]. GPS observations provide evidence of periodic reversals from the ambient direction of relative plate motion suggesting fault slip along the subducting plate interface. Coincident with these innocuous events, seismically observed tremor is observed to correlate both spatially and temporally [*Rogers and Dragert*, 2003]. These tremors are characterized by a lack of high frequency content relative to normal earthquakes of similar size [*Obara*, 2002], which suggests that slip results from a slow, low stress-drop process, probably associated with high pore fluid pressure [*Kao et al.*, 2005].

Each episode, lasting days to weeks, is observed to yield 2 - 3 cm [*Szeliga et al.*, 2008] of the 4cm/yr north-easterly convergence [*Wilson*, 2003] of the subducting Juan de Fuca plate beneath North America. These innocuous events reduce the moment available for high-stress-drop failure in the slow slip region and may hold the key for better understanding the spatial and temporal dynamics of Cascadia subduction. Tighter constraints on the slow slip source region could facilitate better spatial estimates of the freely slipping, transition, and locked segments of the subducting Juan de Fuca plate relative to the dense urban centers along the fault margin. And, because slow slip transfers stress to the seismogenic portion of the plate interface, [e.g. *Rogers and Dragert*, 2003], monitoring transient events may serve in forecasting the threat of a megathrust earthquake by inferring the temporal and spatial variations in the loading of the seismogenic zone.

Increased GPS instrumentation allows for improved imagery of the slow slip region from geodetic inversions. Still, required smoothing limits the resolution of these inversions. As a result, tremor epicenters promise to be the best hope for a high-resolution map of the slow slip region. However, while the recurring spatial and temporal correlation suggests a close link between these two separate phenomena, it does not require their descriptions to be synonyms for the same source process. Nevertheless, in addition to the spatio-temporal correlation between tremor and slow slip [*Rogers and Dragert*, 2003], evidence from low-frequency earthquakes comprising tremor in Japan

[*Shelly et al.*, 2007] and polarization analysis of tremor in Cascadia [*Wech and Creager*, 2007] suggests tremor and slow slip are manifestations of the same shear process. Furthermore, recent tremor and slow slip evidence suggest tremor may serve as a reliable proxy for slow slip activity [*Aguiar et al.*, submitted; *Hiramatsu et al.*, 2008]. Regardless of the ongoing discussion of Cascadia tremor depth and mechanism, if this latter relationship between tremor and slip holds, tremor epicenters provide a high-resolution map of the slow slip region.

Though macroscopic spatial and temporal correlations have been identified [*Rogers and Dragert*, 2003; *Szeliga et al.*, 2008; *McCausland et al.*, 2005], a detailed comparison has not been reported due to the inherent difficulties in locating tremor. Tremor has been successfully located in this region [*Kao et al.*, 2005; *McCausland et al.*, 2005; *Kao et al.*, 2007], but the high costs in computation time or labor associated with these techniques have made producing a complete tremor catalog difficult. Using results from a tremor autodetection and autolocation method [*Wech and Creager*, submitted], we present a complete catalog of thousands of tremor epicenters from the July 2004, September 2005, January 2007 and May 2008 ETS episodes and the February 2007—April 2008 inter-ETS time window. These results strengthen the correlation between slow slip and tremor by creating a high-resolution image of the slow slip region while providing evidence of additional stable sliding outside ETS episodes that may bleed off the remaining strain accumulation in the slow slip region.

2. Seismic Data and Methods

Tremor epicenters were automatically detected and located by employing a cross-correlation method to generate potential epicenters before using the resulting epicenters to detect tremor [*Wech and Creager*, submitted]. By automatically analyzing network coherence through epicentral reliability and spatial repeatability, this method simultaneously locates and obviates the labor-intensive human efforts in detecting tremor. Based on data availability and quality, each ETS episode was analyzed with slightly different data sets. Using data from Pacific Northwest Seismic Network (PNSN) (2004-2008 ETS), Pacific Geoscience Centre (PGC) (2008 ETS), and EarthScope/Plate Boundary Observatory (PBO) borehole seismometers (2005-2008 ETS), and Earthscope CAFE seismometers (2007 ETS), we choose a subnet comprising about 20 stations in western Washington and southern Vancouver Island based on geographic distribution and tremor signal-to-noise ratios.

Locations are estimated with a cross-correlation method that maximizes tremor signal coherency among seismic stations. For a given 5-minute time window of vertical-component data, we bandpass filter from 1—8 Hz, create envelope functions, low-pass filter at 0.1 Hz, and decimate to 1 Hz. We obtain centroid location estimates by cross-correlating all station pairs and performing a 3-D grid search over potential source-location S-wave lag times that optimize the cross correlations [*Wech and Creager*, submitted]. Using bootstrap error analysis and comparisons with earthquake locations we estimate that our epicentral errors are up to 8 km with larger depth errors.

3. Geodetic methods

The growing density of GPS stations allows the distribution of slip from each transient to be formally estimated from GPS deformation [*Szeliga et al.*, 2008]. In this formulation, we specify the plate boundary surface by linearly interpolating between depth contours specified by Fluck et al. [1997]. This surface is then divided into variable sized subfaults whose typical dimensions are around 25 km along strike and 15 km down dip. Exact subfault dimensions vary with geometry. Three dimensional geometry dominated by the bend in the subducting plate mandates that each subfault be independently specified with a unique local strike, dip and rake, in addition to its along-strike and downdip length.

Inverting for slip amounts to solving $Gs = d + \varepsilon$ where G is a Jacobian matrix of Green's functions relating surface displacement to a unit of pure thrust fault slip, s is the vector of dip-slip slip at each subfault, d is the observed vector of north, east and vertical slow-slip event offsets, weighted by their formal uncertainties, for each GPS station recording an event (Table 1), and ε is the error. The number of unknown model parameters greatly exceeds the number of observations so additional information is required to reduce the nonuniqueness and stabilize the inversion. We apply both positivity and solution smoothness constraints in our inversion process [*Szeliga et al*., 2008].

3. ETS tremor descriptions

For each ETS episode only those epicenters with error estimates under 5 km that cluster in space and time are determined to represent tremor [*Wech and Creager*, submitted]. Epicenters are color-coded by time to show migration and are only tracked up to the southern tip of Vancouver Island (Figure 1), after which they are beyond our network coverage. Time scales vary according to the beginning and end of each event. Despite variable station coverage, each episode yielded similar numbers of hours of tremor and number of epicenters (Table 1).

For the July 2004 ETS we detect 174 hours of tremor and 2,774 epicenters.

Tremor began on July 8th in the eastern Strait of Juan de Fuca. Averaging 11 km/day, tremor bursts spread west over the next 7 days throughout the straits to just south of southern Vancouver Island before splitting and heading southeast (ending on July 17th) and northwest (ending about September 23rd) with a late burst occurring in the northern Olympic Peninsula on July 25th (Figure 1).

For the September 2005 ETS we detect 197 hours of tremor and 3,118 epicenters. Tremor began on September 3rd (Figure 1), east of Vancouver Island. During the next ten days at a rate of 12 km/day, tremor bursts migrated to the southwest, stalling beneath the northern shore of the Olympic Peninsula before bifurcating and heading southeast (ending on September 15th) and northwest (ending about September 30th) as seen by *Wech and Creager* [2007].

For the January 2007 ETS we detect 200 hours of tremor and 3,061 epicenters. Migrating at 9 km/day from central Puget Sound to Vancouver Island from January 14th–31st and then North beyond our network's border, with a late burst occurring in southern Puget Sound on January 25th–31st (Figure 1).

For the May 2008 ETS we detect 227 hours of tremor and 3,677 epicenters migrating from central Puget Sound to Vancouver Island from May 4th–24th at 13 km/day and then North beyond our network's border, with a late burst occurring in southern Puget Sound on May 15th–17th (Figure 1).

Tremor migration varies among each episode, but common patterns can be seen between the 2004 and 2005 episodes. In each case, tremor began further downdip prior to an updip, southwest migration that resulted in bifurcation and along strike migration to the north and south. This behavior is markedly different than the migrations of the 2007 and 2008 tremor episodes. Though latitudinally offset by about 20 km, in each of these latter cases tremor initiated in the south Puget Sound region, then migrated northward along strike with a late burst reoccurring in the southern Puget Sound. Overall, each tremor pattern is approximately 20-25 km wide where the plate interface is 30-45 km deep (Figure 1) and migrated at an average of 10-13 km/day (Table 1). The 2007 tremor pattern is notably narrower, which probably more accurately represents true map-view constraints due to the higher data quality of the Earthscope CAFE data set. Epicenters from each episode have a well-resolved sharp updip boundary about 75 km east of current estimates of the downdip edge of the locked zone [*McCaffrey et al.*, 2007] (Figure 1).

4. Tremor and slip

Equipped with a complete catalog of tremor epicenters for each ETS episode, we can compare the tremor source region with slow slip inversions. Combining these new ETS geodetic inversion with complete tremor descriptions enables detailed spatial comparisons between tremor and slip. Figure 2 plots the contours of all tremor epicenters gridded into counts/0.1x0.1 degree bins for individual ETS events and compares these against the results of the slip inversions. For each of the 4 ETS episodes, tremor and slow slip are independently observed to occur in the same areas, with regions of high tremor density spatially correlating extremely well with regions of concentrated slow slip (Figure 2). This comparison confirms previous large-scale spatial correlations in Cascadia, but the increased number of tremor epicenters from a complete catalog confines ETS tremor to the slow slip region while strengthening the case for a close relationship between the two phenomena.

Figure 3 shows contours from the combination of all tremor epicenters from the past 4 ETS episodes and compares this ETS tremor map against the slow-slip sum from the same 4 ETS episodes. This compilation highlights two things. First, unsurprisingly, there is a very strong spatial correlation between the regions of high tremor activity and increased slow slip. Second, the tremor density contours show a very sharp updip boundary in the middle of the Olympic Peninsula. This updip edge is seen more easily with tremor than slip, likely because of the smoothing required for geodetic inversions. Given the varying seismic subnets from episode to episode and the station coverage updip of this edge, the resulting edge is likely a real feature that serves as an ETS boundary that may reflect some change in plate interface conditions. And, because of the uncertainties in tremor epicenters, this boundary may be even sharper than indicated.

5. Inter-ETS Tremor

Monitoring inter-ETS tremor by hand has shown that there are many bursts of tremor with no associated geodetic signal [*McCausland et al., 2005*]; however, there has been very little location work and no complete catalog has yet characterized an inter-ETS time window. Our automated tremor detection and location algorithm afforded the opportunity to perform a detailed tremor study of one inter-ETS period. During the 15 months between the January 2007 and May 2008 ETS episodes, we identify and locate numerous innocuous tremor bursts [*Wech and Creager*, submitted]. We keep the tremor detections with bootstrap errors less than 5 km and that cluster in space and time to avoid noise and earthquakes. We obtain 182 hours of inter-ETS tremor and 2,717 epicenters from the February 2007—April 2008 inter-ETS period (Figure 4). These tremors occur in the slow slip region, spatially compliment ETS tremor (Figure 4), and account for approximately 45% of the tremor detected during the entire ETS cycle [*Wech and Creager*, submitted]. The peak of the distribution of interETS tremor is slightly downdip of the peaks during ETS.

6. Implications

With our tremor catalog we have provided a detailed description of tremor activity in space and time during each of the last 4 ETS episodes and shown new complete evidence of a tight spatial correlation between episodic tremor and slip. Comparing the spatial extent of the tremor source region with slip inversions strengthens the correlation between tremor and slip, and taking this correlation a step further highlights the utility of having a detailed description of tremor.

The tremor and slip spatial correlations of each individual ETS episode and their total accumulations provide strong evidence that tremor can be used to monitor slip. Alone this evidence does not establish a one to one correlation between the two phenomena. However, when put together with previous tremor and slip results from Japan and Cascadia, we argue that our tremor epicenters monitor and map slow slip, even when the amount of slip is below the current GPS detection levels. Evidence from the two most studied ETS regions, southwest Japan and northern Cascadia, suggests in several ways that tremor is a proxy for slip. Estimated seismic moment from Japan tremor and total duration from Cascadia tremor have been observed to be proportional to the size of corresponding slow slip episodes [*Hiramatsu et al*., 2008; *Aguiar et al*., submitted]. Japanese tremor appears to be composed of low-frequency earthquakes that represent thrust on the plate interface during slow slip events [*Shelly et al*., 2007]. In Cascadia analysis of tremor polarization [*Wech and Creager*, 2007] combined with recent tremor depth estimates [*La Rocca et al.*, submitted] lead to the same conclusion. These results combined with our spatial correlations suggest that Cascadia tremor occurs on the plate interface with a thrust mechanism associated with slow slip. Therefore, we interpret tremor and slip as different observations of the same physical process but on opposite ends of the frequency spectrum—a spectrum that is slowly filling in. The time-scale gap between tremor observed at frequencies above 1 Hz and slow slip observed over many days is beginning to be filled in with observations from southwest Japan of slow events radiating energy at periods of 20 seconds [*Ito et al.*, 2007] and 200 seconds [*Ide et al.*, 2008].

This interpretation thus allows us to map the slow slip region and use tremor epicenters to monitor slow slip occurrences. By extrapolating the spatial and temporal correlation between the two phenomena, tremor epicenters can supplement geodetic spatial constraints of the slow slip region. Tremor epicenters provide a high resolution map of the slow slip region, reinforced and quantified by GPS observations.

7. Conclusions

Ultimately this leads us to two important conclusions. First, combining tremor epicenters from all four ETS episodes provides a high-resolution map of the slow slip region (Figure 3) which maps a region of strain release to accommodate the northeasterly 4cm/yr convergence of the subducting Juan de Fuca plate beneath North America. Our epicenters show evidence of a very sharp updip edge to the slow-slip region. We interpret this boundary to represent a change in the physical properties at the plate interface that inhibits updip ETS-like behavior. Second, finding 45% of tremor activity during an ETS cycle to occur between ETS events suggests that the mapped slow slip region is, in the long term, accommodating all of the relative plate motion. With typical slip of 2-3 cm every 14 months, ETS only accounts for 45-65% of the plate convergence rate of 4 cm/yr. The inter-ETS tremor, which we propose represents slip at levels below current GPS resolution, accommodates the remaining strain build up. Of course, we have only had the opportunity to study one inter-ETS period, but inter-ETS bursts have long been observed. Together with the updip edge observed with the past cumulative ETS tremor map and the growing understanding that tremor and slip are the same phenomena, this result implies slow slip occurs in the freely slipping region and tremor epicenters demarcate the downdip edge of the transition zone.

If tremor accommodates all of the converging plate motion, it raises an important question about how stress is released updip of the sharp ETS boundary and downdip of the seismogenic zone. It is possible that slip might be accommodated by coseismic shear failure during a megathrust earthquake, postseismic afterslip associated with a megathrust rupture, large slow slip events with repeat intervals longer than continuous GPS has been available, or a combination of all of these. By further constraining this transition zone with more ETS and inter-ETS observations using increased instrumentation and higher quality data, we can begin to answer this question and better understand the seismic hazards from a megathrust earthquake downdip of the seismogenic zone.

Event	Number of Epicenters	Duration (hrs)	Migration (km/day)	Slip (cm)	M_w
July 2004	2,774	173.7	10.9	2.3	6.6
September 2005	3,118	196.8	11.8	3.1	6.7
January 2007	3,061	199.8	9.4	3.9	6.6
May 2008	3,677	226.7	13.3	2.9	6.5
February 2007—April 2008	2,717	181.5	11.3	NA	NA

Table 1. Tremor location (columns 2-4) and geodetic slip (columns 5-6) information for each ETS episode and one inter-ETS episode.

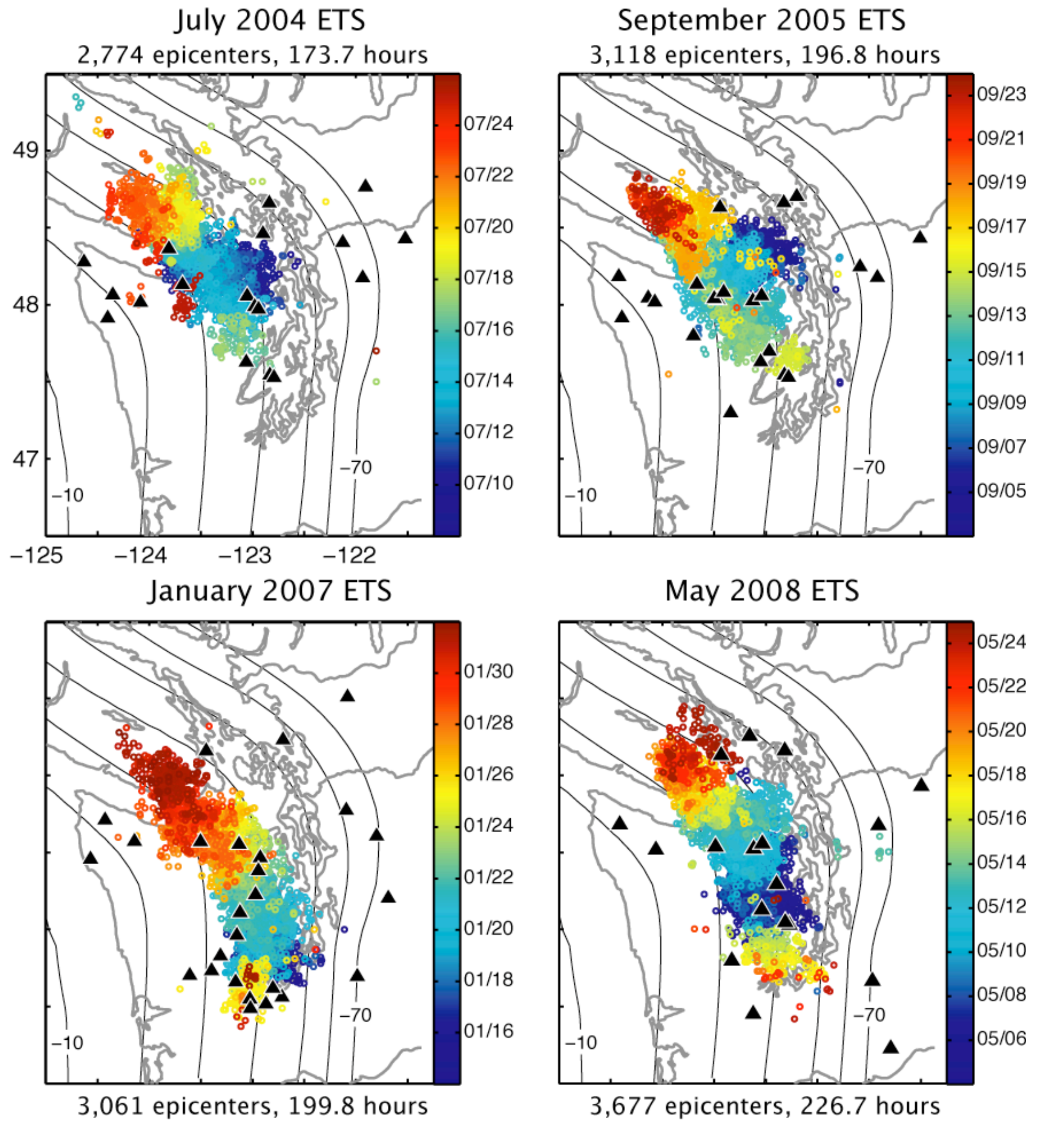

Figure 1. Tremor locations from the 4 ETS episodes showing tremor epicenters (dots color coded by time), station distribution (triangles) and plate interface geometry (contoured at 10-km intervals) from McCrorey et al., [2004].

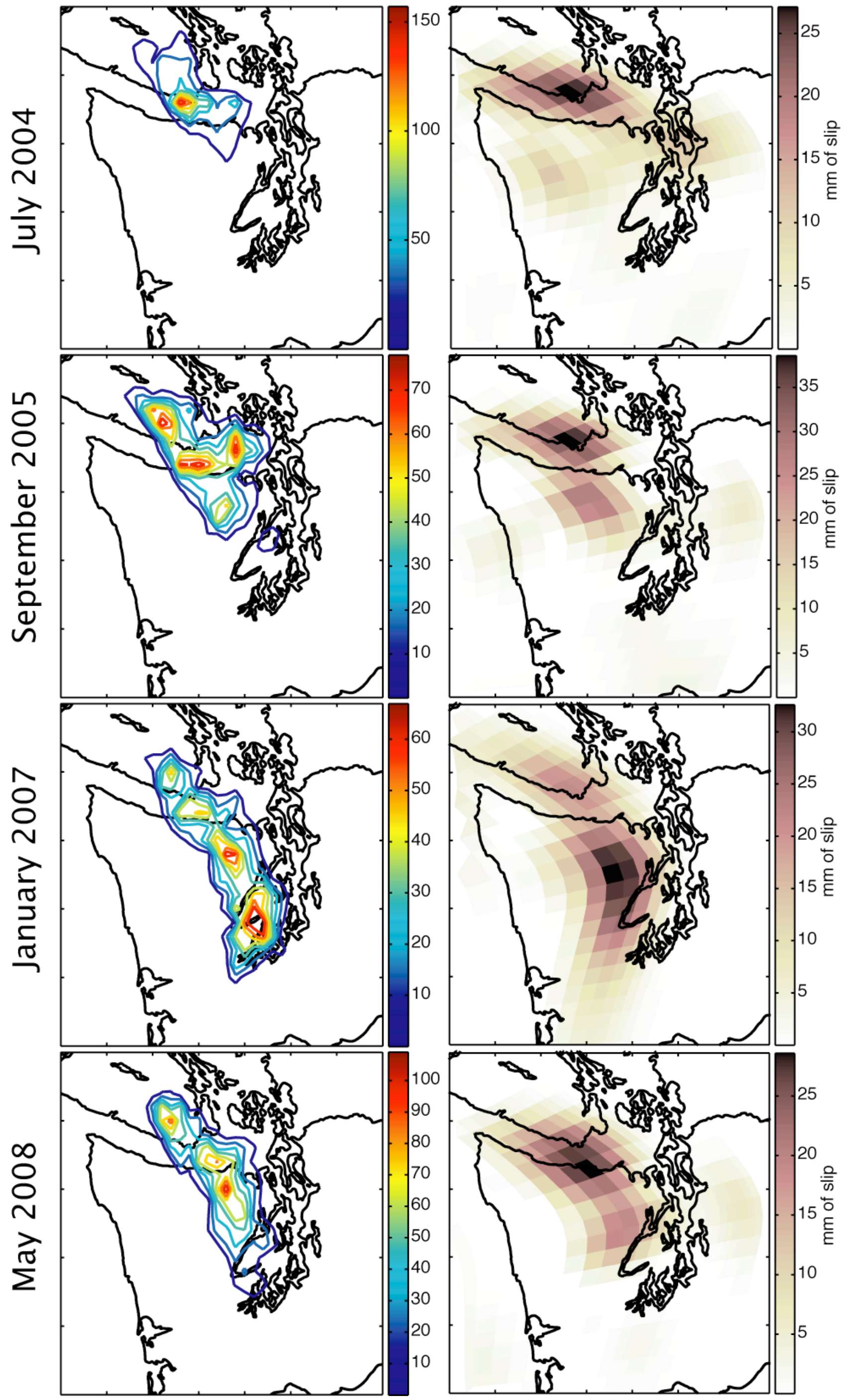

Figure 2. Total tremor contours (left) compared with geodetic slip estimates (right) for each of the 4 most recent ETS episodes. Tremor contours show number of tremor epicenters per 0.1 by 0.1 degree bin.

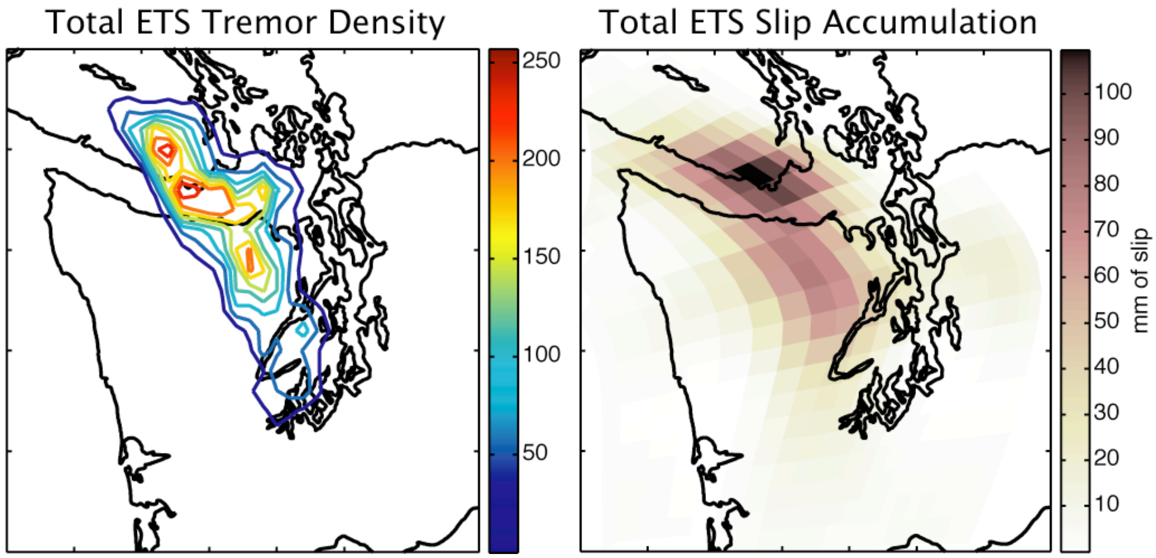

Figure 3. Sum of all tremor epicenters per 0.1 by 0.1 degree bin (left) and of plate-interface slip (right) over 4 ETS episodes.

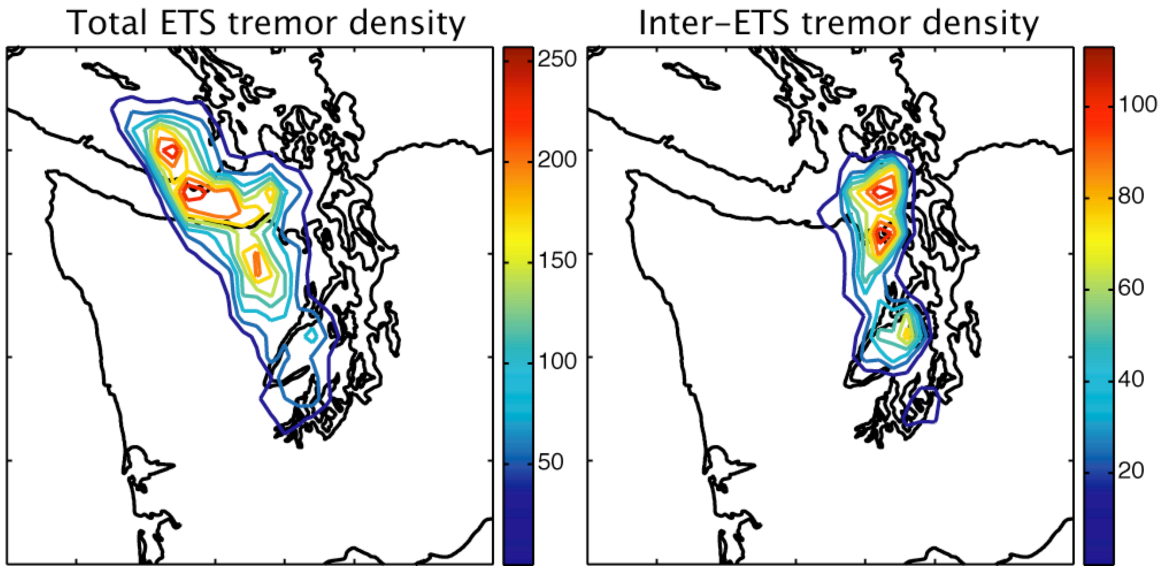

Figure 4. Sum of all tremor epicenters per 0.1 by 0.1 degree bin for all four ETS episodes (left) and for one inter-ETS period (right).

Acknowledgements: This material is based on work supported by the National Science Foundation and the USGS. Primary seismic data were supplied by PNSN, PGC, Earthscope and PBO seismometers. We thank Robert Crosson for his envelope processing. We also thank John Vidale, Justin Rubinstein Weston Thelen and Justin Sweet for valuable discussion.

References

Aguiar, A. C., T. I. Melbourne, and C. Scrivner, Moment rate during Cascadia tremor constrained by GPS, *J. Geophys. Res.*, submitted.

Dragert, H., K. Wang, and T. S. James (2001), A silent slip event on the deeper Cascadia subduction interface, *Science*, 292, 1525-1528, doi:10.1126/science.1060152.

Goldfinger, C., et al. (2003), Holocene earthquake records from the Cascadia subduction zone and northern San Andreas Fault based on precise dating of offshore turbidites., *Annual Review of Earth and Planetary Sciences*, 31, 555–577.

Hiramatsu, Y., T. Watanabe, and K. Obara (2008), Deep low-frequency tremors as a proxy for slip monitoring at plate interface, *Geophys. Res. Lett.*, 35, L13304, doi:10.1029/2008GL034342.

Ide, S., K. Imanishi, Y. Yoshida, G. C. Beroza, and D. R. Shelly (2008), Bridging the gap between seismically and geodetically detected slow earthquakes, *Geophys. Res. Lett.*, 35, L10305, doi:10.1029/2008GL034014.

Ito, Y., K. Obara, K. Shiomi, S. Sekine, and H. Hirose (2007), Slow earthquakes coincident with episodic tremors and slow slip events, *Science*, 315, 503–506.

Kao, H., S. Shan, H. Dragert, G. Rogers, J. F. Cassidy, and K. Ramachandran (2005), A wide depth distribution of seismic tremors along the northern Cascadia margin, *Nature*, 436, 841-844, doi:10.1038/nature03903.

Kao, H., P. J. Thompson, G. Rogers, H. Dragert, and G. Spence (2007), Automatic detection and characterization of seismic tremors in northern Cascadia, *Geophys. Res. Lett.*, 34, L16313, doi:10.1029/2007GL030822.

La Rocca, M., K. C. Creager, D. Galluzzo, S. Malone, J. E. Vidale, J. R. Sweet, A.G.

Wech (2008), Precise location of tremor from high-frequency S-P time difference, *Science*, submitted.

McCaffrey, R., A. I. Qamar, R. W. King, R. Wells, G. Khazaradze, C. A. Williams, C. W. Stevens, J. J. Vollick, and P. C. Zwick (2007), Fault locking, block rotation and crustal deformation in the Pacific Northwest, *Geophys. J. Int.*, 169(3), 1315 – 1340.

McCrory, P. A., J. L. Blair, D. H. Oppenheimer, and S. R. Walter (2004), Depth to the Juan de Fuca slab beneath the Cascadia subduction margin: A 3-D model for sorting earthquakes, *U. S. Geol. Surv. Data Ser.*, 91.

McCausland, W., S. Malone, and D. Johnson (2005), Temporal and spatial occurrence of deep non-volcanic tremor: From Washington to northern California, *Geophys. Res. Lett.*, 32, L24311, doi:10.1029/2005GL024349.

Miller, M. M., T. Melbourne, D. J. Johnson, and W. Q. Sumner (2002), Periodic Slow Earthquakes from the Cascadia Subduction Zone, *Science*, 295, 2423.

Obara, K. (2002), Nonvolcanic Deep Tremor Associated with Subduction in Southwest Japan, *Science*, 296, 1679-1681.

Rogers, G., and H. Dragert (2003), Episodic tremor and slip on the Cascadia subduction zone: The chatter of silent slip, *Science*, 300, 1942 – 1943, doi:10.1126/science.1084783.

Satake, K., K. Wang, and B. F. Atwater (2003), Fault slip and seismic moment of the 1700 Cascadia earthquake inferred from Japanese tsunami descriptions, *J. Geophys. Res.*, 108 (B11), 2535, doi:10.1029/2003JB002521.

Shelly, D. R., G. C. Beroza, and S. Ide (2007), Non-volcanic tremor and low-frequency earthquake swarms, *Nature*, 446, 305-307, doi:10.1038/nature05666.

Szeliga, W., T. Melbourne, M. Santillan, and M. Miller (2008), GPS constraints on 34 slow slip events within the Cascadia subduction zone, 1997 – 2005, *J. Geophys. Res.*, 113, B04404, doi:10.1029/2007JB004948.

Wech, A. G., and K. C. Creager (2007), Cascadia tremor polarization evidence for plate interface slip, *Geophys. Res. Lett.*, 34, L22306, doi:10.1029/2007GL031167.

Wech, A. G., and K. C. Creager (2008), Automatic detection and location of Cascadia tremor, *Geophys. Res. Lett.*, submitted.

Wilson, D. S. (1993), Confidence intervals for motion and deformation of the Juan de Fuca Plate, J. Geophys. Res., 98 (B9), 16,053–16,071.